

Supporting Information

**Photovoltaic-driven solid-state Zn-CO₂ electrochemical cell system
with sunlight-insusceptible chemical production**

Xueyuan Wang, Muhammad Arsalan Ghausi, Rui Yang, Maoxiang Wu, Jiafang Xie,*
Yaobing Wang*

X. Wang, M. A. Ghausi, R. Yang, Prof. M. Wu, Dr. J. Xie, Prof. Y. Wang
CAS Key Laboratory of Design and Assembly of Functional Nanostructures, and
Fujian Key Laboratory of Nanomaterials, Fujian Institute of Research on the Structure
of Matter, Chinese Academy of Sciences, Fuzhou, Fujian 350002, P. R. China

X. Wang, M. A. Ghausi, R. Yang University of Chinese Academy of
Sciences Beijing 100049, P. R. China

*E-mail: xiejiafang@fjirsm.ac.cn, wangyb@fjirsm.ac.cn

Preparation of catalysts

Synthesis of SiNFC. 11 mmol D-glucose (AR, Sinopharm), 120 mmol NH_4F (AR, Sinopharm) and 33 mmol SiO_2 nanoparticles (50 nm, 99.5%, Aladdin) were ground until a uniform mixture was obtained. The mixture was then transported to the furnace tube for pyrolysis under Ar: warming to 900 °C with a rate of 10 °C min^{-1} and maintaining at 900 °C for 1 h. The resulting particles were collected and soaked in 10% HF with stirring for 12 hours to remove SiO_2 template. The remaining precipitate was washed with excessive DI water to obtain neutral solution and then dried overnight in vacuum oven. SiNCIC was prepared by replacing NH_4F with NH_4HCO_3 (99.995%, Macklin). SiNC was prepared without NH_4F .

Characterization

The high-resolution scanning electron microscope (SEM) images were obtained by SU8010. The high angle annular dark field (HAADF) image and elemental distribution were characterized using a transmission electron microscope (TEM, JEOL JEM-2010) at an accelerating voltage of 200 kV. X-ray power diffraction (XRD) patterns were recorded on a MiniFlex 600 diffractometer using a $\text{Cu K}\alpha$ ($\lambda = 1.54 \text{ \AA}$) radiation source at the scan rate of 5° min^{-1} . The element contents and the chemical valence of the materials were analyzed by X-ray photoelectron spectroscopy (XPS, VG ESCALAB 250). Specific correction was performed by employing the C 1s binding energy of 284.6 eV. N_2 sorption isotherms were measured at 77 K using ASAP 2010 analyzer, after the samples were degassed in a vacuum at 120 °C for 12 h. The specific surface area and the pore size distribution were calculated using the Brunauer-Emmett-Teller (BET) model and density function theory (DFT) model, respectively.

Electrochemical measurements

Electrochemical measurements were carried out in a three-electrode system with an electrochemical station (CHI 660E). Ag/AgCl (saturated KCl) and a Pt wire were used as reference and counter electrode, respectively. The double-layer capacitance of materials was evaluated in 0.1 M NaClO_4 (99.5%, Aladdin) saturated with Ar. The

electrochemical CO₂ reduction reaction test was carried out in an H-type reactor with 0.1 M KHCO₃ (99.7%, Sigma-Aldrich) electrolyte separated by a Nafion membrane (Nafion 211, DuPont). Prior to experiments, CO₂ (99.995%) was bubbled through cathodic electrolyte for 20 min and controlled at 20 mL min⁻¹ during experiments. The electrochemical O₂ evolution test was carried out on a rotating ring disk electrode (1600 rpm) in 1 M KOH with 5-mm-diameter electrode. The LSV curve of CDRR and OER were obtained at a scan rate of 10 mV s⁻¹. All potentials in this part were converted to potential vs. the reversible hydrogen electrode (RHE) according to the equation ($E_{\text{RHE}} = E_{\text{Ag/AgCl}} + 0.197 \text{ V} + (0.0591 \times \text{pH}) \text{ V}$).

Liquid-state Zn-CO₂ electrochemical cell test

The liquid-state Zn-CO₂ electrochemical cell test was conducted in a double-electrolyte system separated by a bipolar membrane (TWBP, Astom). The SiNFC catalyst loaded 0.2 mg cm⁻² on the carbon paper (HCP-020, Hesen) was applied as cathode. Zn plate (0.15~0.25 mm, Sinopharm) was applied as anode. The catholyte was 1 M KHCO₃ bubbled with CO₂ and anolyte was 1 M KOH (AR, Sinopharm) added with 0.01 M Zn(CH₃COO)₂ (AR, Sinopharm).

Solid-state Zn-CO₂ electrochemical cell test

The solid-state Zn-CO₂ electrochemical cell test was conducted with SiNFC catalyst loaded on carbon cloth (HCP330N, Hesen) as cathode. Alkaline hydrogel electrolyte was prepared by adding 5 g polyvinyl alcohol (PVA) into 50 mL solution of 1 M KOH and 0.01 M Zn(CH₃COO)₂ at 90 °C. When a uniform solution was got under stirring, it was transported to a glass plate to form the thin film. After repeating the step of frozen at -3 °C for 12 h and then thawed at room temperature for three times, the alkaline electrolyte membrane was obtained. Neutral hydrogel electrolyte was prepared with the similar procedure but replacing KOH and Zn(CH₃COO)₂ by 1 M NaCl. Battery tests were conducted by a cell testing system (CT2001A, LANHE).

Artificial leaf test

The artificial leaf test was conducted by applying three triple-junction GaAs solar cells (each one has the illustration surface of $0.9 \times 0.94 \text{ cm}^2$) to harvest solar energy and drive the charge process of the solid-state Zn-CO₂ electrochemical cell. External resistance was used to adjust device charging voltage and circuit current.

Gas analysis

CO and H₂ generations were detected by a gas chromatography (GC, 9790II, FULI) equipped with a TDX-01 column, a Nickel reformer, a thermal conductivity detector, and a hydrogen ion flame detector.

Efficiency calculation

Faradaic efficiency of CO was calculated by:

$$FE_{CO} = \frac{CO \text{ Volume} \div 22.4 \text{ mol} \cdot L^{-1} \times 2 \times 96485 \text{ C} \cdot \text{mol}^{-1}}{Q_{total}}$$

“2” in the equation is the electron transfer number during every CO molecule generation. The FE calculation of H₂ is similar to that of CO.

Energy efficiency of CO generation from the Zn-CO₂ electrochemical cell was calculated by:

$$EE_{CO} = \frac{\Delta G_{output}}{\Delta G_{input}} = \frac{n \times E_{discharge} \times F + FE_{CO} \times \Delta G_{CO, splitting}}{n \times E_{charge} \times F}$$

CO₂ splitting in the Zn-CO₂ electrochemical cell was calculated based on the heating values of related reduction reaction (Equation 3), $\Delta G^{\theta} = 257.19 \text{ kJ mol}^{-1}$, $F = 96485 \text{ C mol}^{-1}$.

The solar-to-CO efficiency was calculated by:

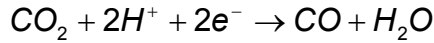
$$SCE_{solar-to-CO} = EE_{CO} \times EE_{solar}$$

in which, EE_{solar} is the energy efficiency of the photovoltaic cell with the value of 20.6%.

Calculation of the theoretical potential of the liquid-state Zn-CO₂ electrochemical cell

When the liquid-state Zn-CO₂ electrochemical cell discharges, the following reactions are assumed to take place:

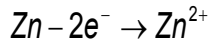
Cathode (1 M KHCO₃ sat. CO₂, pH=7.3):



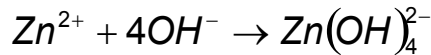
$$E_c = E_{\text{CO}_2/\text{CO}}^\theta - \frac{RT}{nF} \ln \left[\frac{1}{\alpha_{\text{H}^+}^2} \right] = -0.106\text{V} - \frac{8.314 \times 298.15}{2 \times 96485} \ln \frac{1}{(10^{-7.3})^2} = -0.538\text{V}$$

$$E_{\text{CO}_2/\text{CO}}^\theta = -0.106\text{V vs SHE}$$

Anode (1 M KOH with 0.01 M Zn(CH₃COO)₂, pH=14):



Zn²⁺ would react with OH⁻ spontaneously:



When Zn(OH)₄²⁻ is over its solubility:



$$E_a$$

$$= E_{\text{Zn}(\text{OH})_4^{2-}/\text{Zn}}^\theta - \frac{RT}{nF} \ln \left[\frac{\alpha_{\text{OH}^-}^4}{\alpha_{\text{Zn}(\text{OH})_4^{2-}}} \right] = -1.199\text{V} - \frac{8.314 \times 298.15}{2 \times 96485}$$

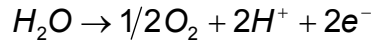
The theoretical potential of discharge process for the liquid-state Zn-CO₂ electrochemical cell:

$$E_{\text{discharge}} = E_c - E_a = -0.538\text{V} - (-1.258\text{V}) = 0.72\text{V}$$

In calculations, R is 8.314 J K⁻¹ mol⁻¹ (molar gas constant), T is 298.15 K, n is 2 (the number of electrons transferred per mole of product), F is 96485 C mol⁻¹ (Faradaic constant), and is the corresponding activity.

When the liquid-state Zn-CO₂ electrochemical cell charges, the following reactions are assumed to possibly take place:

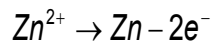
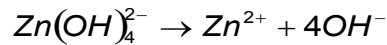
Cathode (1 M KHCO₃ sat. CO₂, pH=7.3):



$$E_c = E_{H_2O/O_2}^\theta - \frac{RT}{nF} \ln \left[\frac{1}{\alpha_{H^+}^2} \right] = 1.229 V - \frac{8.314 \times 298.15}{2 \times 96485} \ln \frac{1}{(10^{-7.3})^2} V = 0.867 V$$

$$E_{H_2O/O_2}^\theta = 1.229 V \text{ vs SHE}$$

Anode (1 M KOH with 0.01 M Zn(CH₃COO)₂, pH=14):



When Zn(OH)₄²⁻ is lower than its solubility:



$$E_a$$

$$= E_{Zn(OH)_4^{2-}/Zn}^\theta - \frac{RT}{nF} \ln \left[\frac{\alpha_{OH^-}^4}{\alpha_{Zn(OH)_4^{2-}}} \right] = -1.199 V - \frac{8.314 \times 298.15}{2 \times 96485}$$

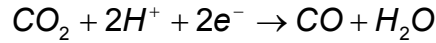
The theoretical potential of charge process for the liquid-state Zn-CO₂ electrochemical cell:

$$E_{charge} = E_c - E_a = 0.867 V - (-1.258 V) = 2.125 V$$

Calculation of the theoretical potential of the solid-state Zn-CO₂ electrochemical cell

When the solid-state Zn-CO₂ electrochemical cell discharges, the following reactions are assumed to take place:

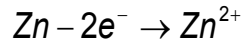
Cathode (1 M NaCl, pH=7):



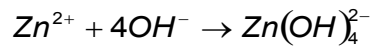
$$E_c = E_{\text{CO}_2/\text{CO}}^\theta - \frac{RT}{nF} \ln \left[\frac{1}{\alpha_{\text{H}^+}^2} \right] = -0.106\text{V} - \frac{8.314 \times 298.15}{2 \times 96485} \ln \frac{1}{(10^{-7})^2} \text{V} = -0.520\text{V}$$

$$E_{\text{CO}_2/\text{CO}}^\theta = -0.106\text{V vs SHE}$$

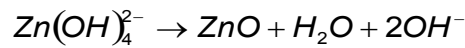
Anode (1 M KOH with 0.01 M Zn(CH₃COO)₂, pH=14):



Zn²⁺ would react with OH⁻ spontaneously:



When Zn(OH)₄²⁻ is over its solubility:



$$E_a$$

$$= E_{\text{Zn}(\text{OH})_4^{2-}/\text{Zn}}^\theta - \frac{RT}{nF} \ln \left[\frac{\alpha_{\text{OH}^-}^4}{\alpha_{\text{Zn}(\text{OH})_4^{2-}}} \right] = -1.199\text{V} - \frac{8.314 \times 298.15}{2 \times 96485}$$

The theoretical potential of discharge process for the solid-state Zn-CO₂ electrochemical cell:

$$E_{\text{discharge}} = E_c - E_a = -0.520\text{V} - (-1.258\text{V}) = 0.738\text{V}$$

When competitive hydrogen evolution occurs:



$$E_c' = E_{\text{H}^+/\text{H}_2}^\theta - \frac{RT}{nF} \ln \left[\frac{1}{\alpha_{\text{H}^+}^2} \right] = 0\text{V} - \frac{8.314 \times 298.15}{2 \times 96485} \ln \frac{1}{(10^{-7})^2} \text{V} = -0.414\text{V}$$

$$E_{\text{H}^+/\text{H}_2}^\theta = 0\text{V vs SHE}$$

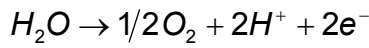
The theoretical potential of discharge process for H⁺/H and Zn²⁺/Zn couple in the solid-state Zn-CO₂ electrochemical cell:

$$E'_{\text{discharge}} = E'_c - E'_a = -0.414 \text{ V} - (-1.258 \text{ V}) = 0.844 \text{ V}$$

In calculations, R is 8.314 J K⁻¹ mol⁻¹ (molar gas constant), T is 298.15 K, n is 2 (the number of electrons transferred per mole of product), F is 96485 C mol⁻¹ (Faradaic constant), and is the corresponding activity.

When the solid-state Zn-CO₂ electrochemical cell charges, the following reactions are assumed to possibly take place:

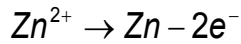
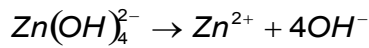
Cathode (1 M NaCl, pH=7):



$$E_c = E_{H_2O/O_2}^\theta - \frac{RT}{nF} \ln \left[\frac{1}{\alpha_{H^+}^2} \right] = 1.229 \text{ V} - \frac{8.314 \times 298.15}{2 \times 96485} \ln \frac{1}{(10^{-7})^2} \text{ V} = 0.885 \text{ V}$$

$$E_{H_2O/O_2}^\theta = 1.229 \text{ V vs SHE}$$

Anode (1 M KOH with 0.01 M Zn(CH₃COO)₂, pH=14):



When Zn(OH)₄²⁻ is lower than its solubility:



$$E_a$$

$$= E_{Zn(OH)_4^{2-}/Zn}^\theta - \frac{RT}{nF} \ln \left[\frac{\alpha_{OH^-}^4}{\alpha_{Zn(OH)_4^{2-}}} \right] = -1.199 \text{ V} - \frac{8.314 \times 298.15}{2 \times 96485}$$

The theoretical potential of charge process for the solid-state Zn-CO₂ electrochemical cell:

$$E_{\text{charge}} = E_c - E_a = 0.885 \text{ V} - (-1.258 \text{ V}) = 2.143 \text{ V}$$

Supplementary figures

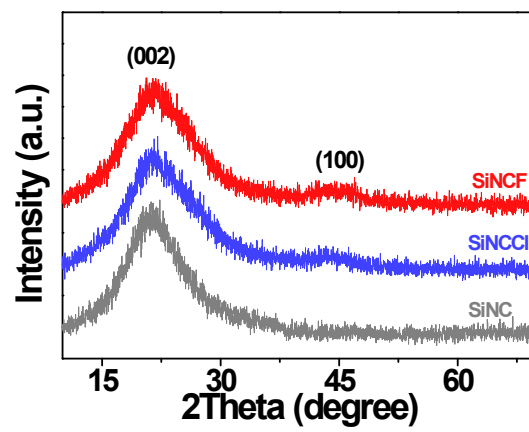


Fig. S1. XRD spectra of SiNFC, SiNCIC, and SiNC samples.

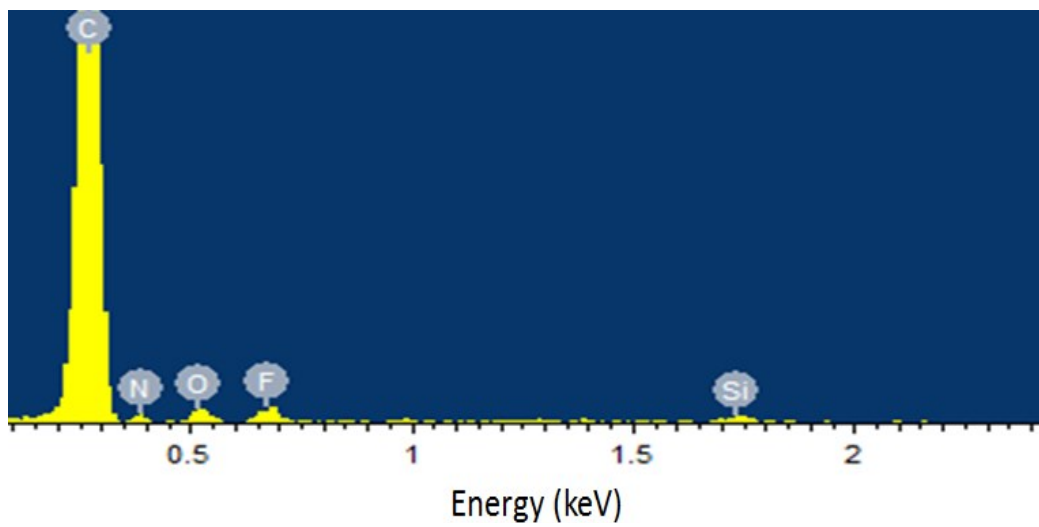


Fig. S2. EDX spectrum of SiNFC.

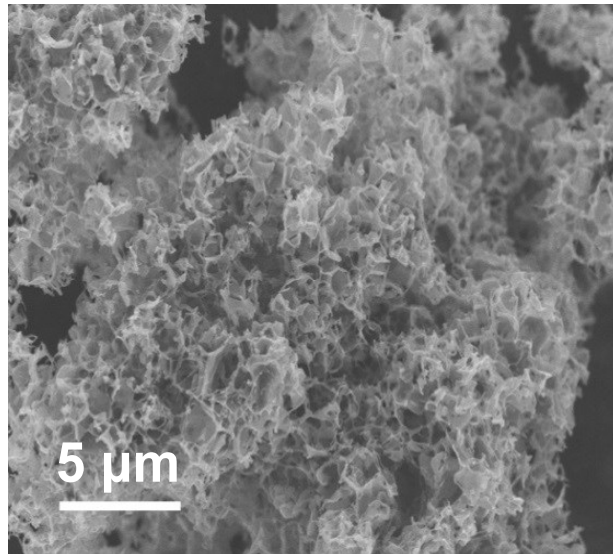


Fig. S3. SEM image of SiNFC.

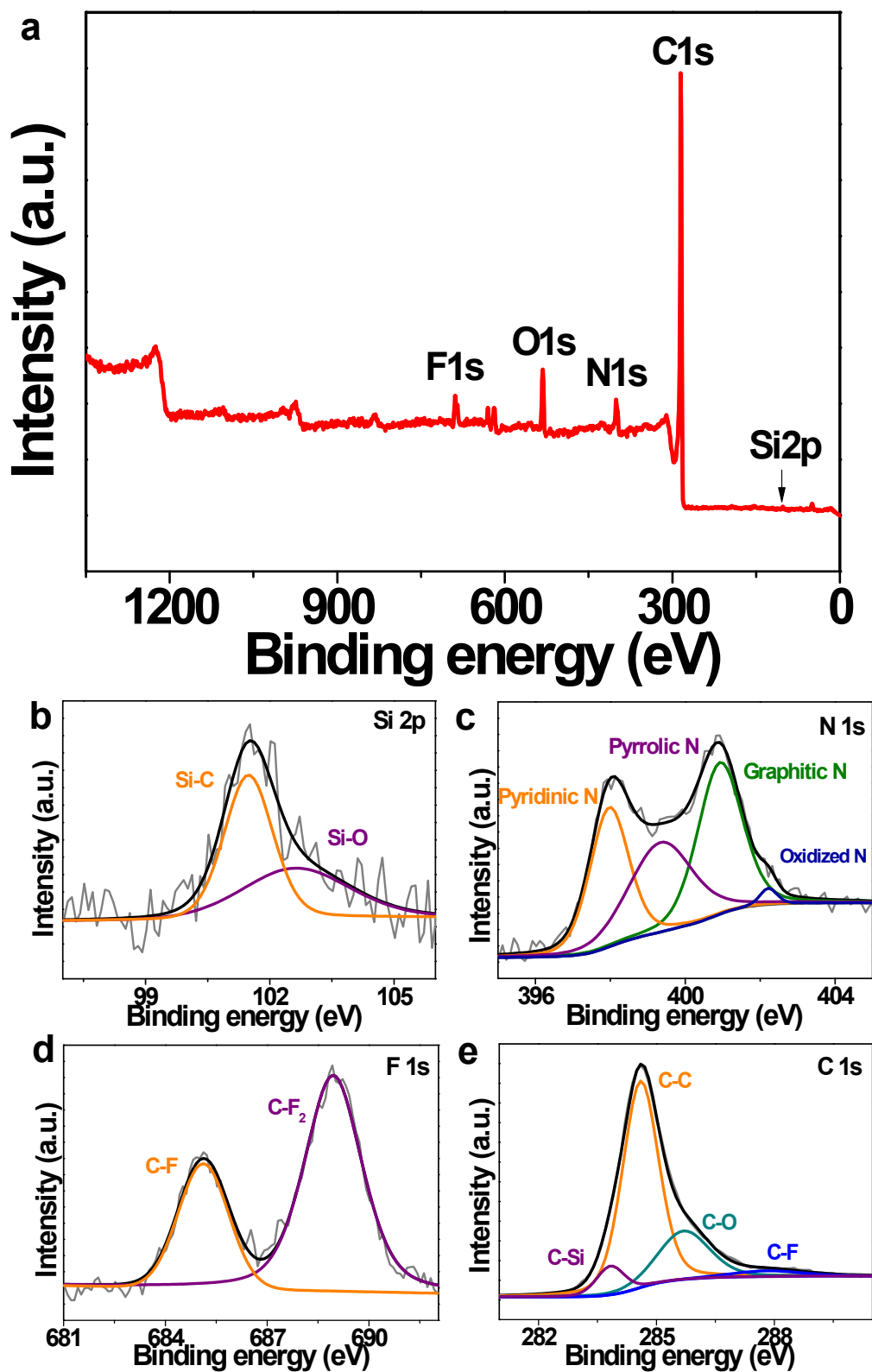


Fig. S4. XPS spectra of SiNFC. (a) Survey spectrum. High-resolution spectra for (b) Si, (c) N, (d) F, and (e) C elements.

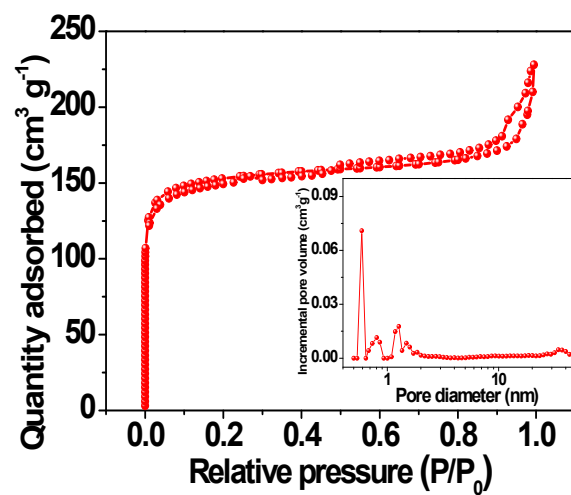


Fig. S5. N₂ adsorption-desorption isotherms and (inset) pore size distribution of SiNFC.

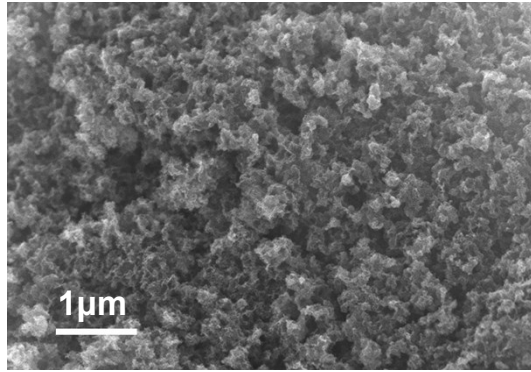


Fig. S6. SEM image of SiNCIC.

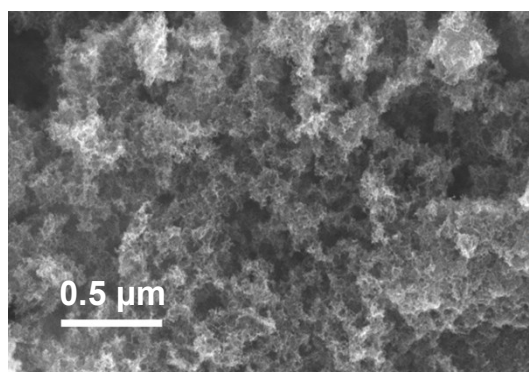


Fig. S7. SEM image of SiNC.

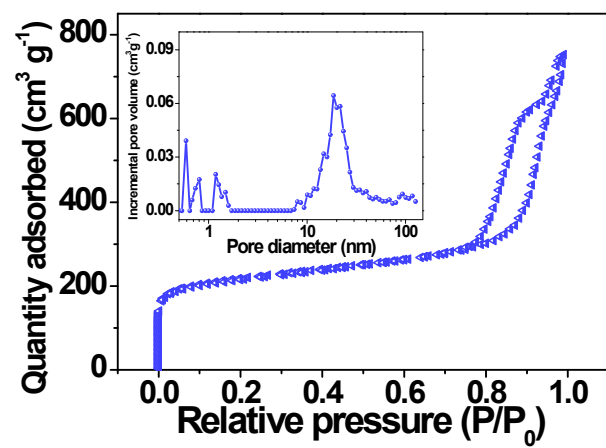


Fig. S8. N₂ adsorption-desorption isotherms and (inset) pore size distribution of SiNCIC.

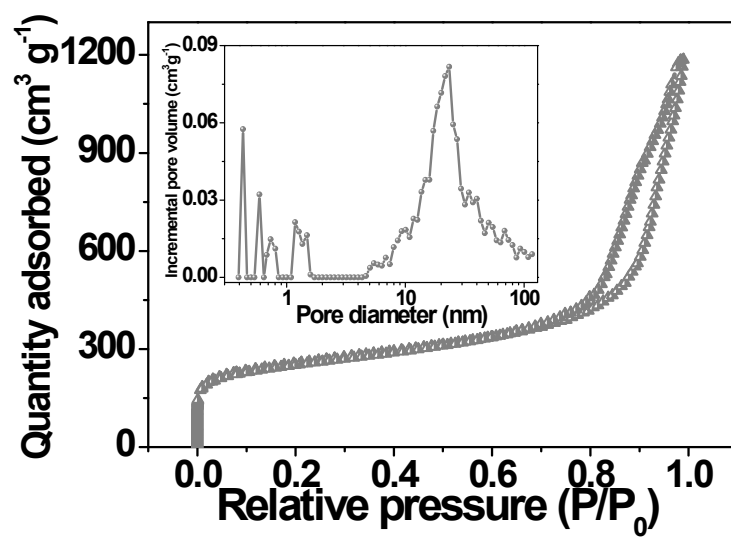


Fig. S9. N₂ adsorption-desorption isotherms and (inset) pore size distribution of SiNC.

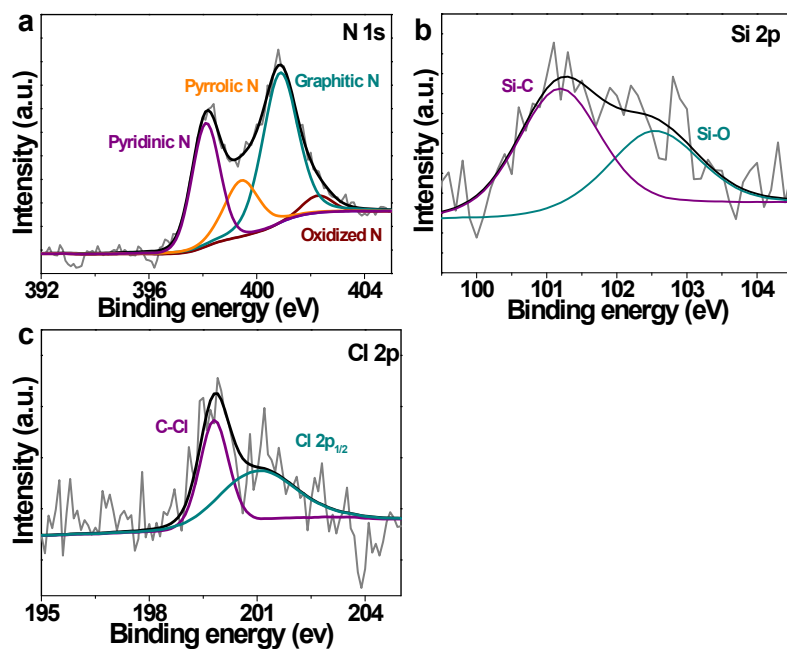


Fig. S10. XPS spectra of SiNFC. High-resolution spectra for (a) N, (b) Si, and (c) Cl elements.

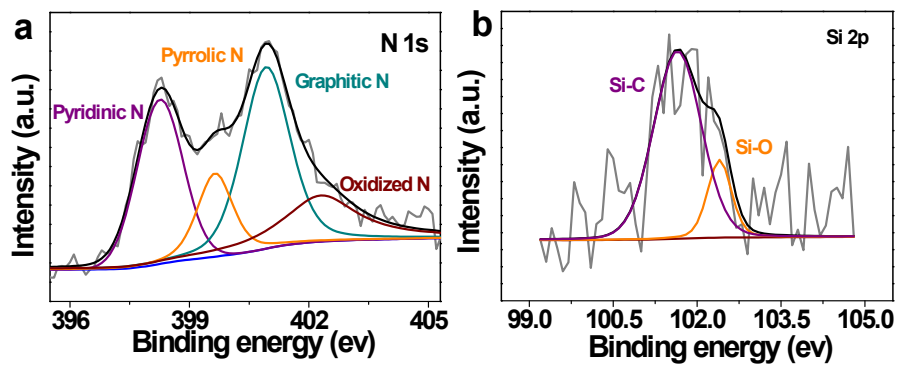


Fig. S11. XPS spectra of SiNFC. High-resolution spectra for (a) N and (b) Si elements.

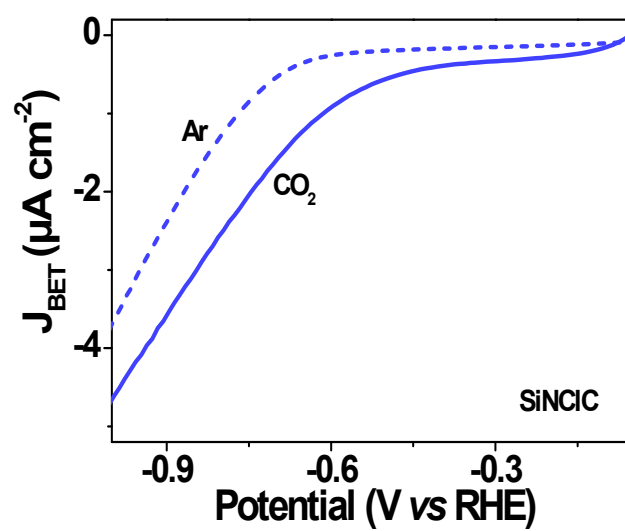


Fig. S12. LSV curves of SiNCIC in CO_2 and Ar conditions. Scan rate: 10 mV s^{-1} .

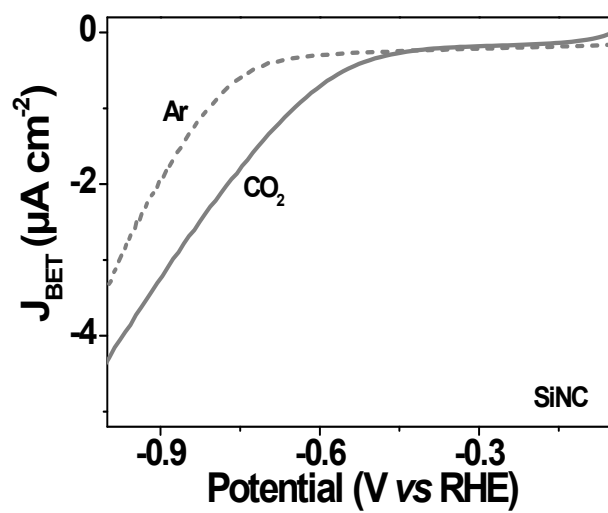


Fig. S13. LSV curves of SiNC in CO_2 and Ar conditions. Scan rate: 10 mV s^{-1} .

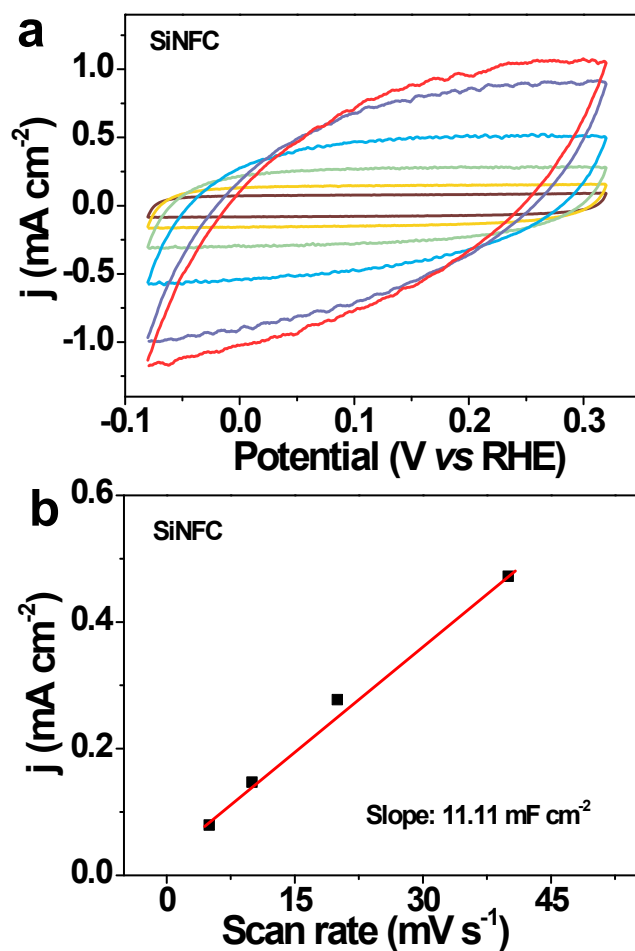


Fig. S14. Double-layer capacitance (C_{dl}) calculation of SiNFC. (a) Scan rate dependence cyclic voltammetry. (b) Peak current of the cyclic voltammogram as a function of scan rate. Scan Rates: 5 mV, 10 mV, 20 mV, 40 mV, 80 mV, and 100mV. Electrolyte: 0.1 M NaClO_4 .

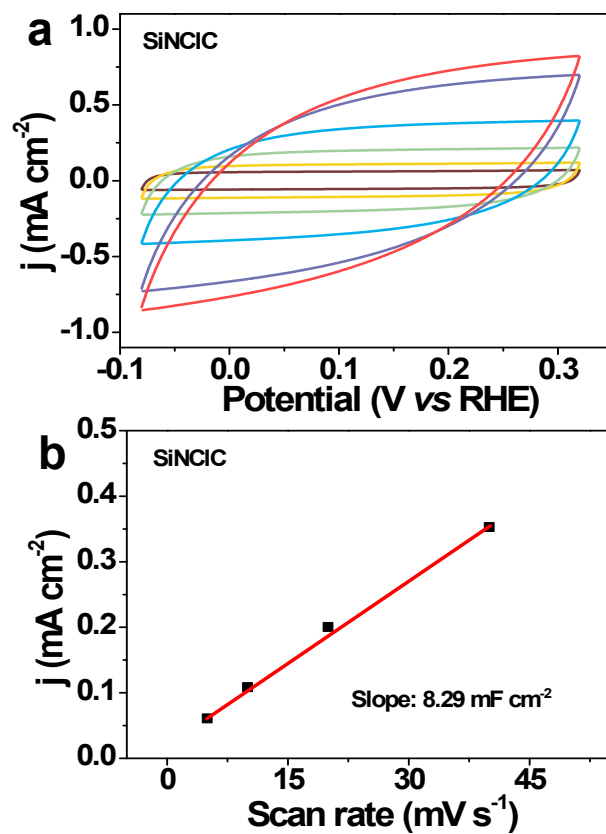


Fig. S15. C_{dl} calculation of SiNCIC. (a) Scan rate dependence cyclic voltammetry. (b) Peak current of the cyclic voltammogram as a function of scan rate. Scan Rates: 5 mV, 10 mV, 20 mV, 40 mV, 80 mV, and 100mV. Electrolyte: 0.1 M NaClO_4 .

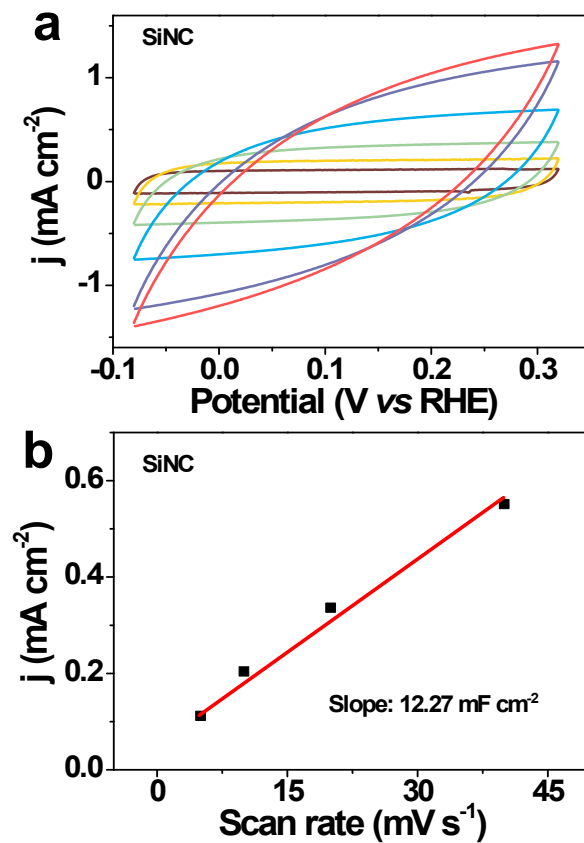


Fig. S16. C_{dl} calculation of SiNC. (a) Scan rate dependence cyclic voltammetry. (b) Peak current of the cyclic voltammogram as a function of scan rate. Scan Rates: 5 mV, 10 mV, 20 mV, 40 mV, 80 mV, and 100mV. Electrolyte: 0.1 M NaClO_4 .

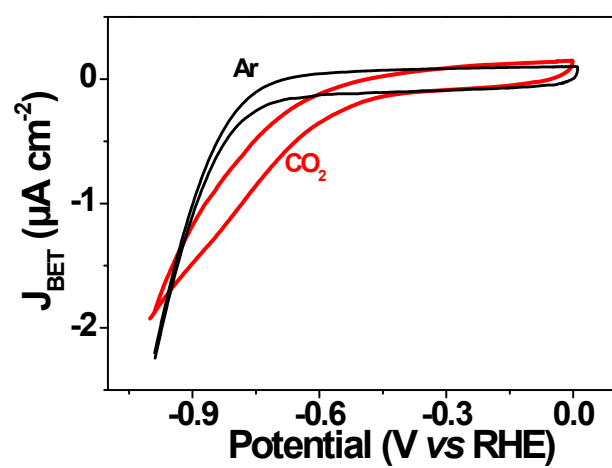


Fig. S17. Cyclic voltammetry curve of SiNFC in 0.1M KHCO₃ saturated with CO₂ and 0.1 M NaClO₄ saturated with Ar. Scan rate: 10 mV s⁻¹. BET area instead of geometric area was applied to calculate current densities here.

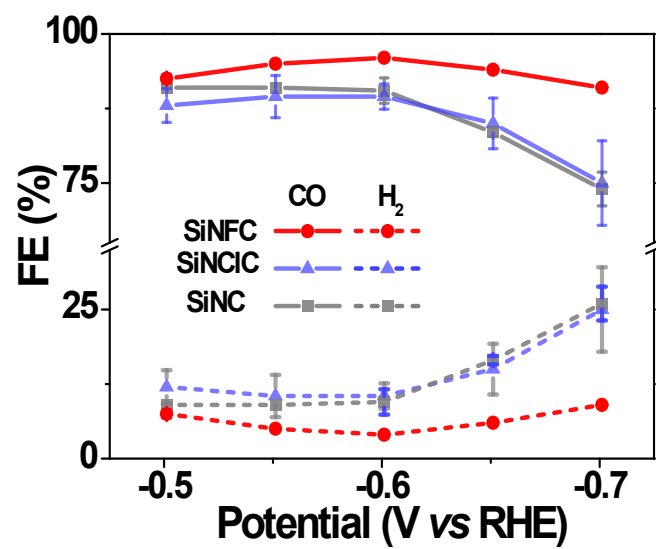


Fig. S18. FEs of CO and H₂ generation in potentiostatic electrolysis on SiNFC, SiNC, and SiNCIC.

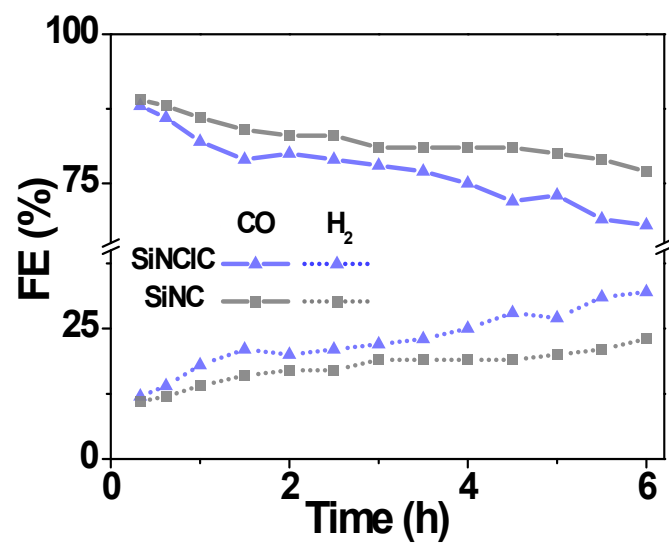


Fig. S19. FEs of CO and H₂ generation in 6-h electrolysis at -0.6 V on SiNC and SiNCIC.

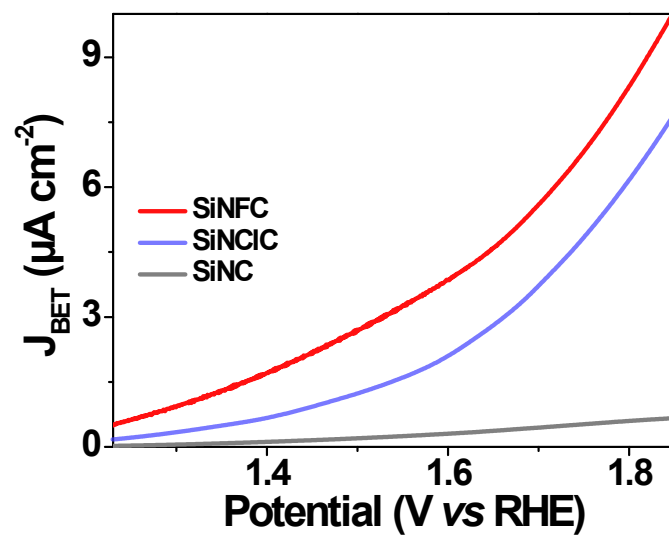


Fig. S20. LSV curve of SiNFC in 1 M KOH. Scan rate: 10 mV s^{-1} . Specific surface area was applied to calculate current density. Results of SiNC and SiNCIC were also shown.

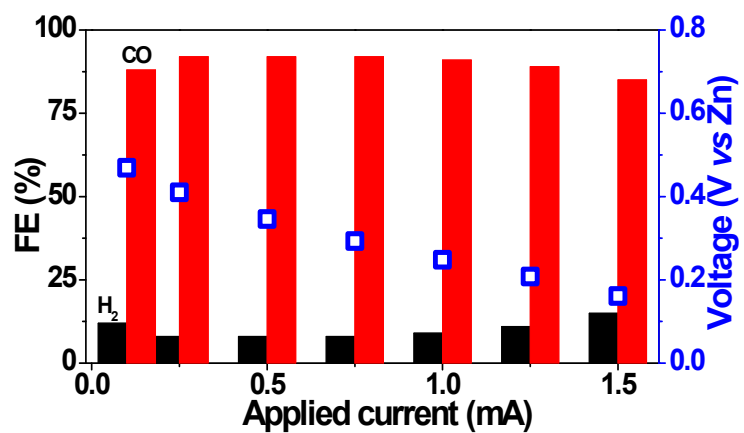


Fig. S21. Gas products distribution and potential of liquid-state Zn-CO₂ electrochemical cells at several discharge currents.

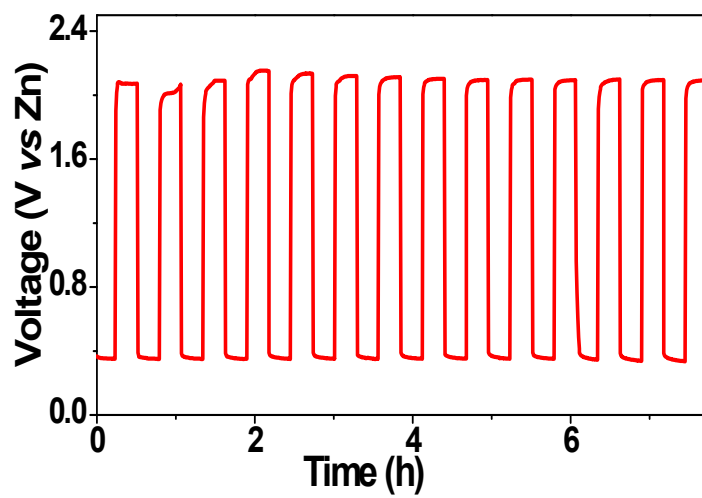


Fig. S22. Galvanostatic discharge-charge cycling of liquid-state Zn-CO₂ electrochemical cells at 0.5 mA.



Fig. S23. Photos of the solid-state Zn-CO₂ electrochemical cells.

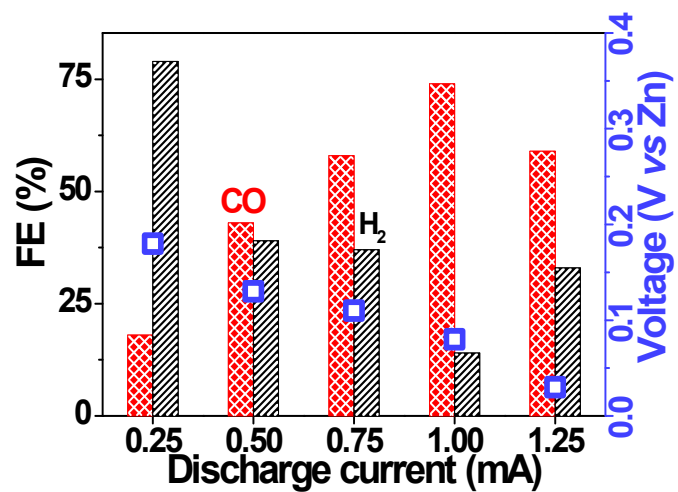


Fig. S24. Products FE and potential of the solid-state Zn-CO₂ electrochemical cell at several discharge currents.

Supplementary Tables

Table S1. BET Surface Area and Pore Volume of SiNFC, SiNCIC, and SiNC

Catalysts	SiNFC	SiNCIC	SiNC
BET Surface Area / m ² g ⁻¹	586.2	799.8	921.1
Pore Volume / cm ³ g ⁻¹	0.35	1.16	1.83

Table S2. Comparison of new artificial leaf with reported artificial photosynthesis devices including artificial leaves.

Catalyst	Photovoltaic cell (Solar-to-electricity efficiency)	Product	Solar-to-product efficiency	Reference
Metal-free SiNFC	Triple-junction GaAs solar cell (21.6%)	CO	15.2%	This work
NiMoZn and Co	Triple-junction amorphous silicon solar cell (7.7%)	H ₂	4.7%	<i>Science</i> ¹
NiMoZn and NiBi	Crystalline silicon solar cell (19.5%)	H ₂	10.2%	<i>PNAS</i> ²
WSe ₂ /IL and Co	PV-a-si-3jn cell (6.0%)	CO	4.6%	<i>Science</i> ³
NiCo ₂ O ₄ /NCNT/CP	Perovskite PV (10%)	H ₂	6.2%	<i>Adv. Energy Mater.</i> ⁴
Ni/Pt and Ni-Pt-Ni _{0.9} Fe _{0.1} O	Perovskite cell (15.16%)	H ₂	10.64%	<i>Adv. Mater.</i> ⁵
Au and IrO ₂	Perovskite photovoltaics (13.4%)	CO	6.5%	<i>Nat. Comm.</i> ⁶

CuAg and IrO ₂	Si solar cell (not mentioned)	H ₂ , CO, C ₁ -C ₃ (hydrocarbon and oxygenate)	8.4%	<i>Energy Environ. Sci.</i> ⁷
NiN-GS and Li ⁺ -tuned Co ₃ O ₄	GaInP ₂ /GaAs/Ge TJ solar cell (27.2%)	CO	12.7%	<i>Chem</i> ⁸
SnO ₂ modified CuO	GaInP/GaInAs/Ge photovoltaic (28.5%)	H ₂ , CO	14.4%	<i>Nature Energy</i> ⁹
Au and NiFe	InGaP/GaAs/Ge solar cell (37.9%)	CO	15.6%(16.4%) ^a	<i>Nat. Comm.</i> ¹⁰
Metal-free SiNC	Polycrystalline Si solar cell (16.6%)	H ₂ , CO	12.5%	<i>Angew. Chem. Int. Ed.</i> ¹¹
DN-CuO	Perovskite solar cell (18.5%)	C ₂ H ₄ , C ₂ H ₆	2.3%	<i>PNAS</i> ¹²
Ni-SNG and N-TiO ₂	Silicon PIN photodiode (18%)	H ₂ , CO	13.6%	<i>Angew. Chem. Int. Ed.</i> ¹³
Anodized silver and Sr ₂ GaCoO ₅	GaInP/GaInAs/Ge (28.5%)	CO	13.9%	<i>Nat. Comm.</i> ¹⁴

^a: 15.6% was obtained with the redox medium and 16.4% was obtained without the redox medium.

References:

1. S. Y. Reece, J. A. Hamel, K. Sung, T. D. Jarvi, A. J. Esswein, J. J. H. Pijpers and D. G. Nocera, *Science*, 2011, **334**, 645-648.
2. C. R. Cox, J. Z. Lee, D. G. Nocera and T. Buonassisi, *Proc. Natl. Acad. Sci. U.S.A.*, 2014, **111**, 14057-14061.
3. M. Asadi, K. Kim, C. Liu, A. V. Addepalli, P. Abbasi, P. Yasaei, P. Phillips, A. Behranginia, J. M. Cerrato, R. Haasch, P. Zapol, B. Kumar, R. F. Klie, J. Abiade, L. A. Curtiss and A. Salehi-Khojin, *Science*, 2016, **353**, 467.
4. T. Sharifi, C. Larsen, J. Wang, W. L. Kwong, E. Gracia-Espino, G. Mercier, J. Messinger, T. Wagberg and L. Edman, *Adv. Energy Mater.*, 2016, **6**, 1600738.
5. S. Kim, T. Kim, S. Lee, S. Baek, T. Park and K. Yong, *Adv. Mater.*, 2017, **29**, 7.
6. M. Schreier, L. Curvat, F. Giordano, L. Steier, A. Abate, S. M. Zakeeruddin, J. Luo, M. T. Mayer and M. Grätzel, *Nat. Commun.*, 2015, **6**, 7326.
7. G. Gurudayal, J. Bullock, D. F. Srankó, C. M. Towle, Y. Lum, M. Hettick, M. C. Scott, A. Javey and J. Ager, *Energy Environ. Sci.*, 2017, **10**, 2222-2230.
8. K. Jiang, S. Siahrostami, A. J. Akey, Y. Li, Z. Lu, J. Lattimer, Y. Hu, C. Stokes, M. Gangishetty, G. Chen, Y. Zhou, W. Hill, W.-B. Cai, D. Bell, K. Chan, J. K. Nørskov, Y. Cui and H. Wang, *Chem*, 2017, **3**, 950-960.
9. M. Schreier, F. Héroguel, L. Steier, S. Ahmad, J. S. Luterbacher, M. T. Mayer, J. Luo and M. Grätzel, *Nature Energy*, 2017, **2**, 17087.
10. Y. H. Wang, J. L. Liu, Y. F. Wang, Y. G. Wang and G. F. Zheng, *Nat. Commun.*, 2018, **9**, 5003.
11. M. A. Ghausi, J. Xie, Q. Li, X. Wang, R. Yang, M. Wu, Y. Wang and L. Dai, *Angew. Chem. Int. Ed.*, 2018, **57**, 13135-13139.
12. T. N. Huan, D. A. D. Corte, S. Lamaison, D. Karapinar, L. Lutz, N. Menguy, M. Foldyna, S. H. Turren-Cruz, A. Hagfeldt, F. Bella, M. Fontecave and V. Mougél, *Proc. Natl. Acad. Sci. U.S.A.*, 2019, **116**, 9735-9740.
13. H. Zhang, J. Ming, J. Zhao, Q. Gu, C. Xu, Z. Ding, R. Yuan, Z. Zhang, H. Lin, X. Wang and J. Long, *Angew. Chem. Int. Ed.*, 2019, **58**, 7718-7722.
14. L. Q. Zhou, C. Ling, H. Zhou, X. Wang, J. Liao, G. K. Reddy, L. Deng, T. C. Peck, R. Zhang, M. S. Whittingham, C. Wang, C.-W. Chu, Y. Yao and H. Jia, *Nat. Commun.*, 2019, **10**, 4081.